ChemComm

Accepted Manuscript

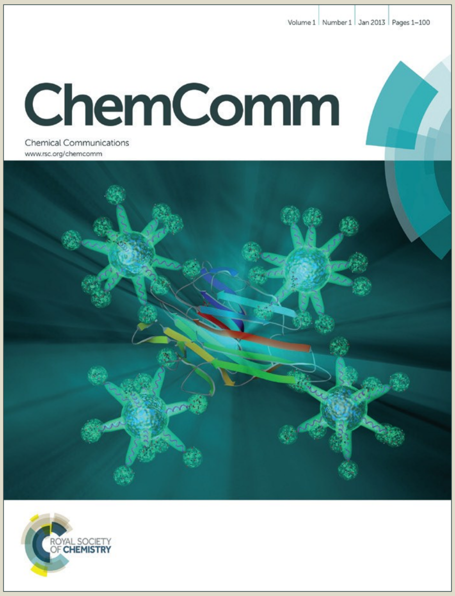

Cite this: DOI: 10.1039/c0xx00000x

www.rsc.org/xxxxxx

ARTICLE TYPE

Composite of Li-Mg-N-H as H_2 storage materials: a case study with $Mg(NH_2)_2$-4LiH-$LiNH_2$

Biswajit Paik, [a] **Hai-Wen Li,** *[a,b] **Jianhui Wang**[a,c] **and Etsuo Akiba**[a,b,d]

Received (in XXX, XXX) Xth XXXXXXXXX 20XX, Accepted Xth XXXXXXXXX 20XX

DOI: 10.1039/b000000x

A reversible hydrogen storage capacity of ~7 wt% at ~150 °C without releasing ammonia can be achieved by mechanically activated three-component composite of $Mg(NH_2)_2$-4LiH-$LiNH_2$.

The state-of-the-art reversible hydrogen storage materials for the on-board application can only offer either of the two: a very suitable hydrogen release at room temperature with poor H_2 storage capacity (example: $LaNi_5H_6$); or, a high hydrogen storage capacity with unacceptably high hydrogen release temperature (example: MgH_2).[1] The major challenge in bridging these two objectives, viz., having acceptable hydrogen storage capacity (typically > 6wt%) and the dehydrogenation within the fuel-cell operating temperature (< 85 °C) comes mainly in the form of unsuitable thermodynamics of the dehydrogenation reactions, especially, in the light weight hydrides.[1, 2] Numerous attempts have been made with the light weight hydrides including amides, borohydrides, alanates, etc[3-5] to develop the H_2 storage materials that can satisfy the critical thermodynamic parameters for the storage material to be rechargeable under the practical conditions. To develop materials that can satisfy the target H_2 storage properties, we attempt to explore the dehydrogenation properties of the Li-Mg-N-H system in the form of composites which are prepared using $Mg(NH_2)_2$, LiH and $LiNH_2$. The advantage of using three starting components, instead of two, to prepare the composite is the flexibility to alter the relative concentrations of the Mg, Li and N in the composites which offer a number of structural features that may help to alter the thermodynamics of the hydrogen uptake/release for the Li-Mg-N-H systems. Some of these advantageous structural features, especially, related to the amide/imide systems include a stable fcc sublattice of N atoms that does not change upon hydrogen sorption, no significant change in the recombination of chemical bonding, etc resulting in an easy facile transformation between amide and imide.[3, 4, 6] These unique features of amide/imide structures that may facilitate a lower dehydrogenation temperature than the other ionic light weight hydrides may be further explored by altering the concentration of Mg^{2+} and Li^+ to fine-tune the dehydrogenation thermodynamics of the composites utilizing the similar size but different charge states of Mg^{2+} and Li^+ ions present in the system.[3-5] Here we report for one selected composite $Mg(NH_2)_2$-4LiH-$LiNH_2$ to show that it is possible to achieve the dehydrogenation thermodynamics which can reversibly store > 7 wt% H_2 having decomposition temperature around 150 °C without losing nitrogen from the system in the form of ammonia. The study is an evidence that a combination of binary amide/imide systems may offer new dehydrogenation properties as, in the present case, the $Mg(NH_2)_2$-4LiH-$LiNH_2$ composite, which may be viewed as a combination of two different H_2 storage systems of $Mg(NH_2)_2$-2LiH and $LiNH_2$-2LiH, does not exclusively follow the decompositions of either of them.

As a part of the experiment, we prepare the composite by ball-milling for 20 h a mixture of commercially available $Mg(NH_2)_2$, LiH and $LiNH_2$ in a mole ratio of 1:4:1 under the inert gas (Ar) environment. The thermal decomposition properties of the composite were carried out by the Thermogravimetry combined with Differential Thermal Analysis and Mass-spectroscopy (TG-DTA-MS). The structural evolution of the crystalline phases by the decomposition was studied by XRD. The dehydrogenation thermodynamics of the composite was studied by the pressure-composition isotherm (PCT). Further details of these experimental procedure and analysis methods are given in the footnote‡.

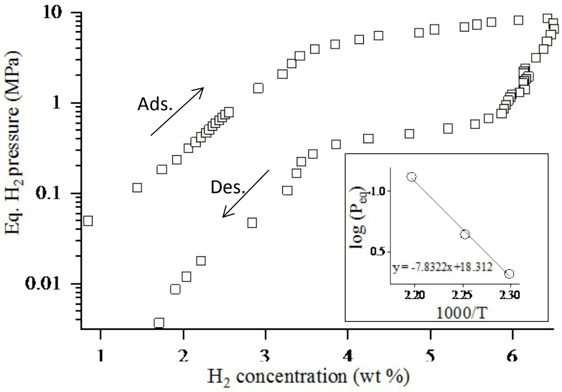

Fig. 1: Pressure-composition isotherm of the $Mg(NH_2)_2$-4LiH-$LiNH_2$ composite at 170 C. (Inset) van't Hoff plot for the composite for dehydrogenation (equilibrium H_2 pressure P_{eq} is in atm and T in Kelvin).

To characterize the dehydrogenation thermodynamics of the composite, we estimate the change of reaction enthalpy (ΔH) and entropy (ΔS) using the van't Hoff equation, shown in Fig.1, by fitting the plateau pressures measured at 160, 170 and 180 °C by the PCT study. The estimated ΔH is 65 kJ·(mole H_2)$^{-1}$ and ΔS is 152 J·(K·mole H_2)$^{-1}$ giving the decomposition temperature T_r for

1 bar H_2 equilibrium pressure (using the relation $\Delta H = T_r.\Delta S$) to be ~154 °C. Comparing the thermodynamics of the composite with those of some other promising amide/imide systems for storing hydrogen, we notice that the $Mg(NH_2)_2$-4LiH-LNH_2 composite has lower decomposition temperature in comparison with the $LiNH_2$-LiH system (ΔH= 66 kJ·(mole H_2)$^{-1}$ and T_r ~ 275 °C).[3] On the other hand, the present composite shows higher decomposition temperature than that of the $Mg(NH_2)_2$-2LiH system (T_r ~ 90 °C) but offers a larger H_2 storage capacity of (7 wt% vs. 5.5 wt%). A large hysteresis between the adsorption and desorption isotherm is notable in the $Mg(NH_2)_2$-4LiH-LNH_2 composite, as was also reported with the $Mg(NH_2)_2$-2LiH.[4]

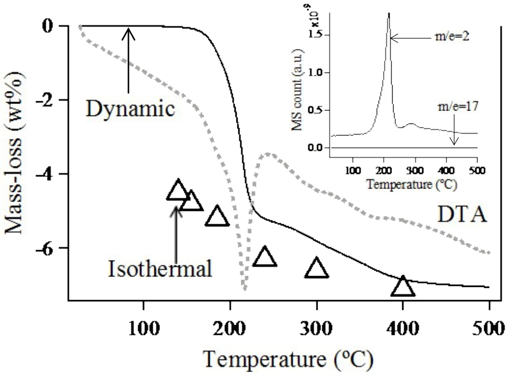

Fig.2: TG-DTA profiles of dynamic (after the 1st cycle) and isothermal mass-loss (as-milled) for $Mg(NH_2)_2$-4LiH-$LiNH_2$ composite. (Inset): Mass spectra of m/e=2 and 17 corresponding to the dynamic heating (5 °C/min).

To further understand the decomposition as a result of gradually releasing hydrogen from the composite, we show (Fig. 2) the TG mass-loss profile of the composite (after 1st H_2 cycle) under the dynamic heating (5 °C/min) up to a temperature of 500 °C together with the mass-loss data obtained by the isothermal decompositions at some selected temperatures. The isothermal mass-losses at temperatures > 200 °C are in the range of 6-7 wt%. These values, as expected, closely resemble the amount of H_2 adsorbed in the PCT study. The released H_2 gas does not contain impurities including ammonia, revealed by the MS profiles of m/ e= 2 (H_2) and 17 (NH_3), also shown in Fig. 2. The reversibility of the reaction in the $Mg(NH_2)_2$-4LiH-$LiNH_2$ composite is confirmed by identifying the phases after hydrogenation of the composite (by the PCT) at ~ 8 MPa H_2 pressure. The phases in the hydrogenated composite, identified by the XRD, are $Mg(NH_2)_2$, $LiNH_2$ and LiH as shown in Fig.3 which also displays the XRD profiles obtained from the as-milled composite (A in Fig. 3) and from the solid residues after dehydrogenating at 180 and 500 °C denoted, respectively, as B and C in Fig.3. Raman spectrum of the composite, after the re-hydrogenation, also confirms the recovery of the characteristic N-H vibrations of $Mg(NH_2)$ and $LiNH_2$ (supplementary information).

The structural change by the dehydrogenation reactions can be further appreciated from Fig.3 which reveals that the as-milled composite is dominated by cubic phases (especially, 2θ values around 30° and 50°) which may include a number of possible non-stoichiometric $LiNH_2$ phases $Li_{1+x}NH_{2-x}$($x \geq 0.02$).[7] Except for the LiH, no characteristics peaks of the other starting compounds, viz., orthorhombic $Mg(NH_2)_2$ or tetragonal $LiNH_2$ have been clearly detected in the pattern A. However, the XRD pattern B (dehydrogenated at 180 °C) clearly shows $Li_{2.6}MgN_2H_{1.4}$ (P-4_3m, space group # 215)[8] along with the cubic reflections (non-stoichiometric phases of $LiNH_2$ assigned as $Li_{1+x}NH_{2-x}$) and a relatively weaker LiH compared to that in the pattern A. At higher temperature (pattern C in Fig. 3), the ternary hydride $Li_{2.6}MgN_2H_{1.4}$ and LiH no longer exist; instead, the nitride LiMgN (probably, forming first a simple cubic disorder antifluorite phase, followed by a cation-ordered orthorhombic phase by structure stabilization at elevated temperature)[9] are formed along with cubic phase that match closely Li_2NH reflections. Combining these information of the structural evolution, we may visualize the dehydrogenation reactions in the following set of chemical reactions (Eq.1- Eq.3):

$Li_2Mg(NH)_2 + (8/3)LiH \rightarrow Li_{2.6}MgN_2H_{1.4} + (8/3)H_2$ (Eq.1)
$LiH + LiNH_2 \rightarrow Li_2NH + H_2$ (Eq.2)
$Li_{2.6}MgN_2H_{1.4} + (1/3)LiH \rightarrow 2Li_2NH + LiMgN + (1/3)H_2$ (Eq.3)

The over-all balance of equation, therefore, is:

$Mg(NH)_2 + 4LiH + LiNH_2 \rightarrow 2Li_2NH + LiMgN + 4H_2$ (Eq.4)

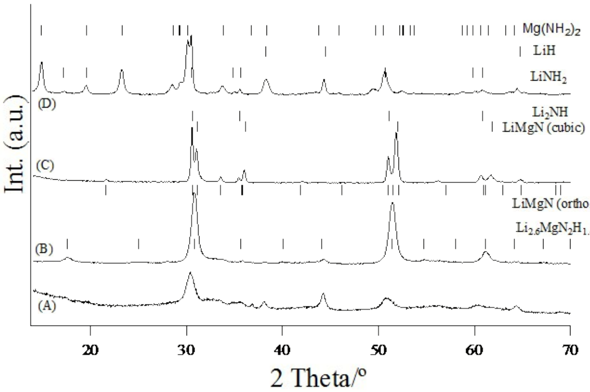

Fig. 3: XRD profiles of $Mg(NH_2)_2$-4LiH-$LiNH_2$ composite: (A) as-milled; (B) after dehydrogenated at 180 °C; (C) after dehydrogenated at 500 °C; (D) after re-hydrogenation at 160 °C.

The left-hand side of equation 4 represents the molar compositions of the starting material; the imide and the nitride in the right-hand side of this equation are the phases identified in the solid residue after the dehydrogenation. The neat expected mass-loss given by equation 4 is 7.2 wt%, a value which is closely satisfied by the dynamic mass-loss of ~ 7.1 wt% (Fig. 2) also indicates that > 90% dehydrogenation reaction may be achieved within 240 °C since the mass-loss by the dynamic/isothermal dehydrogenation at ~240 °C is in the range of 6.6-6.80 wt% (Fig. 2). It may be noted that Eq.1-3 are based on the decomposition reactions of two-component systems and are referred here only as a tool to simplify the complexity of the decomposition reactions in the three-component composite. In fact, equation 1 may be a multi-step reaction, starting with $Mg(NH_2)$ and 2LiH to form $Li_2Mg(NH)_2$ via a two-step reaction.[10] Subsequently, each mole of $Li_2Mg(NH)_2$ interacts with 1/3 mole of LiH to become $Li_{2.6}MgN_2H_{1.4}$. This decomposition pathway is notably different from the reports on some Li-Mg-N-H systems, especially, with similar molar combination of the LHS of Eq.1 yielding L_2NH and Mg_3N_2 as the solid residues ($Mg(NH)_2 + (8/3)LiH \rightarrow 4Li_2NH + Mg_3N_2 + 8H_2$).[11] The stable unary nitrides Mg_3N_2 and Li_3N, reported by these two-component amide/imide systems have not been detected in the dehydrogenated composite in our study; instead, a binary nitride LiMgN has been formed by releasing hydrogen from $Li_{2.6}MgN_2H_{1.4}$, as we suggest in Eq.3, also forming Li_2NH. Since we observe only one distinct plateau in the PCT of the composite, whereas, a series of decomposition reactions are plausible, we believe that these reactions might have taken place as closely sequenced overlapped processes that is expected to release ideally ~7.2 wt% H_2 at ~150 °C. The DTA profile of the dynamical decomposition (Fig.2) also shows one large dip below 250 °C supporting the above assumption that the primary mass-loss (H_2 release) takes place mainly as a single event.

Following the above observation, we assign the inability to fully dehydrogenate the composite around 150 °C as the kinetic barrier of the decomposition reactions (estimated activation energy E_a is ~ 134 $kJ\cdot(mole)^{-1}$, see Fig. S3 in supplementary information) which may be rate-limited by a combination of phase-boundary and nucleation controlled solid-state reactions at the early stage of H_2 release followed by the diffusion-controlled reactions (see Table S1 in supplementary information). These known kinetic barriers for the amide/imide systems[12], however, may be lowered by using, for example, nanoconfinement[13] which may enable the composite to release enough H_2 in a few minutes instead of hours, especially at temperatures < 140 °C without using catalyst (see Fig. S2 in supplementary information).

Despite the kinetic issue, the present study points towards the possibility of an important aspect in tailoring new reaction thermodynamics by altering the relative concentrations of the Li, Mg and N in the physical mixture of a combination of known two-component sub-systems (for example, in this study, the two sub-systems are $2LiH\text{-}Mg(NH_2)_2$ and $2LiH\text{-}LiNH_2$) paving new reaction pathway that may offer a better over-all decomposition thermodynamics than the two-component amide/imide (sub-) systems. In contrast to the limited number of known Li-Mg-N-H systems composed of two components, this approach may open up enormous possibility to design new composites. However, it will be of great interest to know how many of them result in new/novel dehydrogenation reactions. We here report one such combination for the three-component composite of $Mg(NH_2)_2\text{-}4LiH\text{-}LNH_2$ as a typical case study.

We gratefully acknowledge Prof. P. Chen from Dalian Institute of Chemical Physics, P.R. China for numerous suggestions and discussions. The grants under the "Hydrogen Utilization Technology Development" and the "Feasibility Study on Advanced Hydrogen Storage Materials for Automotive Applications (2012)" by the NEDO, Japan are also acknowledged.

Notes and references

[a] *International Research Centre for Hydrogen Energy, Kyushu University, Fukuoka, Japan. E-mail: paik.biswajit.882@m.kyushu-u.ac.jp*
[b] *International Institute for Carbon-Neutral Energy Research (WPI-I2CNR), Kyushu University, Fukuoka, Japan. E-mail: li.haiwen.305@m.kyushu-u.ac.jp*
[c] *Department of Chemical System Engineering, The University of Tokyo, Tokyo, Japan. E-mail:well.wjh@gmail.com*
[d] *Faculty of Engineering, Mechanical Engineering, Kyushu University, Fukuoka, Japan. E-mail:e.akiba@mech.kyushu-u.ac.jp*

† Electronic Supplementary Information (ESI) available: See DOI: 10.1039/b000000x/

‡ The composite was prepared by mixing commercially available $Mg(NH_2)_2$ (HydroLabo, Japan; purity 95%), LiH (particle size 50 µm, Alfa Aesar) and $LiNH_2$ (98% purity, 200 mesh, Aldrich) in a mole ratio 1:4:1. The powders were ball milled by planetary ball-milling machine (10 stainless steel balls with ball-to-powder mass ratio 30:1) for 20 h at 400 rpm under Ar gas. Identification of phases present in the as-milled powders were carried out by powder X-ray diffraction with Cu Ka radiation (Rigaku Ultima IV) and by the Raman spectroscopy (Raman-11 VIS-SS) using blue laser of 532 nm wavelength in a point scan mode. The decomposition properties of the as-milled powders were carried out by thermogravimetry and differential thermal analysis (TG-DTA) using Rigaku Thermoplus-Evo II (TG 8120). Mass-spectroscope (Anelva) was attached with the TG-DTA to simultaneously monitor the evolved gas species. Powder sample (typically 3-5 mg) was taken in an aluminium pan and heated under the He atmosphere (200 ml/min) from RT (~ 25 ºC) to 500 ºC with a heating rate of 5°C/min for the dynamic decomposition. The isothermal decompositions were studied by the TG at the selected temperatures ranging from140-400 °C. A fast heating of 20 °C/min was used in raising the sample temperature to the target temperatures and were maintianed for 2-12 h until the mas-loss profiles reached the equilibrium. The thermodynamic parameters were studied by the PCT apparatus (JMC, Japan). Typically, around 300 mg of powder sample was taken in the PCT tube immersed in the oil bath to maintain the temperature of the sample inside (160, 170 and 180 °C). The PCT data was recorded when the dehydrogenated powder (dehydrogenated under vacuum for ~12 h) was hydrogenated with high purity H_2 increasing the H_2 pressure upto 8 MPa followed by dehydrogenation (H_2 pressure < 0.001 MPa) until no further release of H_2. The delay time for each data point was 2-5 h. The activation energy of the decomposition reaction was studied by the DSC (Thermo plus2 DSC8230HP AEMK) with different heating rate (2, 5, 10 and 20 °C/min) under high purity He atmosphere (0.1 MPa). The temperatures corresponding to the DSC peak of the endothermic reactions, from the four runs, were fitted into the linear form of Kissinger equation to estimate Ea of the decomposition reactions. All the samples, as well as TG and DSC equipments, were kept in glove boxes filled with purified running Ar gas to maintain oxygen level < 1 ppm. Special sample transfer boxes were used for transferring powder samples between the glove boxes and to the Raman spectrometer as well as to the XRD apparatus.

1 A. Züttel, *Naturwissenschaftan*, 2004, **91**, 157.
2 M. Dornheim, S. Doppin, G. Barkhordarian, U. Boesenberg, T. Klassen, O. Gutfleisch, R. Bormann, *Scripta Mat.*, 2007, **56**, 841; H.H. Van Mal, K.H.J. Buschow, A.R. Miedema, *J. Less-Comm. Metal*, 1974, **35**, 65.
3 P. Chen, Z. T. Xiong, J. Z. Luo, J. Y. Lin and K. L. Tan, *Nature*, 2002, **420**, 302.
4 Z. Xiong, G. Wu, J. Hu, P. Chen, *Adv. Mat.*, 2004, **16**, 1522
5 J. Wang, H-W. Li, P. Chen, *MRS Bull.*, 2013, **38**, 480; S. Orimo, Y. Nakamori, J. R. Eliseo, A. Zuttel, C. M. Jensen, *Chem Rev.*, 2007, **107**, 4111; W. Grochala, P.P. Edwards, *Chem. Rev.*, 2004, **104**, 1283; A. R. Akbarzadeh, V. Ozolinš, C. Wolverton, *Adv. Mat.*, 2007, **19**, 3233; W. Luo, *J. Alloys Compd.*, 2004, **381**, 284.
6 T. Noritake, H. Nozaki, M. Aoki, S. Towata, G. Kitahara, Y. Nakamori, S. Orimo, *J. Alloys Compd.*, 2005, **393**, 264; R. Juza, K. Opp, *Z. Anorg. Allg. Chem.*, 1951, **266**, 325; A. Borgschulte, M. O. Jones, E. Callini, B. Probst, S. Kato, A. Züttel, W. I. F. David, S. Orimo, *Energy Environ. Sc.*, 2012, **5**, 6823.
7 W. I. F. David, M. O. Jones, D. H. Gregory, C. M. Jewell, S. R. Johnson, A. Walton, P. P. Edwards, *J. Amer. Chem. Soc.*, 2007, **129**, 1594.
8 Y. Nakamura, S. Hino, T. Ichikawa, H. Fujii, H.W. Brinks, B.C. Hauback, *J. Alloys Compd.*, 2008, **457**, 362.
9 H. Yamane, T. H. Okabe, O. Ishiyama, Y. Maseda, M. Shimada, *J. Alloys Compd.*, 2001, **319**, 124.
10 W. Luo, S. Sickafoose, *J. Alloys Compd.*, 2006, **407**, 274.
11 H. Leng, T. Ichikawa, H. Fujii, *J. Phys. Chem. B*, 2006, **110**, 12964; Y. Nakamori, G. Kitahara, K. Miwa, N. Ohba, T. Noritake, S. Towata, S. Orimo, *J. Alloys Compd.*, 2005, **404-406**, 396.
12 Y. Liu, K. Zhong, K. Luo, M. Gao, H. Pan, Q. Wang, *J. Amer. Chem. Soc.*, 2009, **131**, 1862; P. Chen, Z. Xiong, L. Yang, G. Wu, W. Luo, *J. Phys. Chem. B*, 2006, **110**, 14221.

13 G. Xia, Y. Tan, D. Li, Z. Guo, H. Liu, Z. Liu, X. Yu, *Sci. Rep.*, 2014, **4**, 6599; G. Xia, D. Li, X. Chen, Y. Tan, Z. Guo, H. Liu, Z. Liu, X. Yu, *Adv. Mat.*, 2013, **25**, 6238; R. Demir-Cakan, W.S. Tang, A. Darwiche, R. Janot, *Energ. Environ. Sci.*, 2011, **4**, 3625.